

Implementation of Liouville space search algorithm on strongly dipolar coupled nuclear spins

T. Gopinath and Anil Kumar

NMR Quantum Computing and Quantum Information Group.

Department of Physics, and NMR Research Centre.

Indian Institute of Science, Bangalore - 560012, India.

Liouville space search algorithm [Bruschweiler, Phys. Rev. Lett. **85**, 4815(2000).] utilizes mixed initial states of the ensemble, and has been successfully implemented earlier in weakly coupled spins, in which a spin can be identified as a qubit. It has recently been demonstrated that n-strongly coupled spins can be collectively treated as an n-qubit system. Application of algorithms in such systems, requires new approaches using transition selective pulses rather than qubit selective pulses. This work develops a modified version of Liouville space search algorithm, which is applicable for strongly as well as weakly coupled spins. All the steps of the algorithm, can be implemented by using transition selective pulses. Experimental implementation is carried out on a strongly dipolar coupled four qubit system.

1. INTRODUCTION

An important aspect of information processing is to search a specific data stored in a database [1]. Classical computer operates on binary codes, any number or symbol is represented by combination of bits which can have the value either '0' or '1' [2, 3]. To search an object from N objects, a classical computer must carry out $O(N)$ operations [1]. A quantum computer is based on the principle of quantum superposition, which offers the opportunity to perform parallel computations [4, 5]. Grover search algorithm which uses quantum superposition, finds the marked object in $O(\sqrt{N})$ operations [6]. Most of the

quantum algorithms, including Grover search algorithm, use a pure state (pseudo pure state in NMR) as an initial state [1, 4, 6, 7].

An alternative paradigm for computing has been suggested by Madi, Bruschiweiler, and Ernst, which is based on the mixed states of ensemble, which are represented by density operators in the Liouville space [8]. Mixed states describe a statistical ensemble of spins, rather than individual spins, so that each element of the ensemble performs part of the computation, in the same way as each processor in a classical parallel computer [1]. Bruschiweiler proposed a novel search algorithm, that operates on mixed states in spin Liouville space, and requires $\log_2 N$ queries to search a single object from N unsorted objects [9]. The advantage of Liouville space computation is the use of an input state which is linear combination of different classical input states. Protopopescu had applied Liouville space search to the global optimization problem, and achieved exponential speed-up [10, 11]. Liouville space search algorithm of Bruschiweiler, considers only weakly coupled spins, in which mixed states are represented by linear combination of direct product states of spin polarization operators. The algorithm has been successfully implemented on weakly coupled systems by Xiao et al [12, 13, 14, 15].

Most of the NMR Quantum information processing (QIP) experiments have utilized systems having indirect spin-spin couplings (scalar J couplings) [16, 17]. Since these couplings are mediated via the covalent bonds, the number of coupled spins and hence the number of qubits is limited to a few qubits. Another approach is to use direct dipole-dipole couplings between the spins which are larger in magnitude. In liquids the dipolar couplings are averaged to zero due to rapid isotropic reorientations of the molecules and in rigid solids there are too many couplings yielding broad lines [18]. In molecules partially oriented in anisotropic media, like liquid crystals, one obtains partially averaged intra molecular dipolar couplings with only a finite number of dipolar coupled spins, yielding finite number of sharp NMR resonances [19]. However in such cases often the dipolar couplings are large or comparable to chemical shifts differences between the homonuclear coupled spins, leading to

spins becoming strongly coupled. The method of spin selective pulses and J evolution used in NMR-QIP of weakly coupled spins (liquid state NMR-QIP), leads to complications in strongly coupled spins because of $\vec{I}_i \cdot \vec{I}_j$ terms in the Hamiltonian [18]. However it has been demonstrated that the 2^n non degenerate energy levels system can be collectively treated as an n-qubit system, similar to the case of quadrupolar nuclei oriented in liquid crystal [19, 20, 21]. The manipulation of the states of the qubit are then carried out by using transition selective pulses. Several gates and algorithms have been implemented in such systems [19, 20, 21, 22, 23, 24, 25].

In this work, we generalize the Liouville space search algorithm such that it can be implemented in strongly as well as weakly coupled spins. Experimental implementation is carried out on a four qubit system obtained by strongly dipolar coupled protons of 2-chloro, iodo benzene oriented in ZLI-1132 liquid crystal [22, 25]. In section (2) we explain Liouville space search algorithm, in section (3) we explain the modified version, section (4) contains the experimental implementation, and conclusions are given in section (5).

2. LIOUVILLE SPACE SEARCH ALGORITHM

Liouville space search algorithm finds a marked object in 2^n unsorted objects, which correspond to 2^n eigen states [9]. The eigen states in weakly coupled spins, are same as product states obtained from individual spin sates, and the corresponding density matrices are obtained from direct product of spin polarization operators [18],

$$\begin{aligned}\psi &= |\alpha\beta\alpha\dots\dots\alpha\rangle = |\alpha\rangle|\beta\rangle|\alpha\rangle\dots\dots|\alpha\rangle \\ \sigma &= |\psi\rangle\langle\psi| = I_1^\alpha I_2^\beta I_3^\alpha \dots\dots I_n^\alpha,\end{aligned}\tag{1}$$

where $I_1^\alpha I_2^\beta I_3^\alpha \dots\dots I_n^\alpha$ is the direct product of polarization operators I_k^α, I_k^β , defined as,

$$\begin{aligned}
I_k^\alpha &= |\alpha_k\rangle\langle\alpha_k| = \frac{1}{2}(\mathbb{1}_k + 2I_{kz}) = \begin{pmatrix} 1 & 0 \\ 0 & 0 \end{pmatrix} \\
I_k^\beta &= |\beta_k\rangle\langle\beta_k| = \frac{1}{2}(\mathbb{1}_k - 2I_{kz}) = \begin{pmatrix} 0 & 0 \\ 0 & 1 \end{pmatrix}.
\end{aligned} \tag{2}$$

$2I_{kz}$ is the Pauli matrix σ_z and $\mathbb{1}_k$ is unity operator of the subspace of spin I_k . In Eq. (1) σ has the dimension of 2^n and it's matrix elements in the eigen basis (also known as Zeeman basis or product basis) are all zero except for one diagonal element belonging to the state $|\alpha\beta\alpha\dots\dots\alpha\rangle$ with coefficient 1, which represents the population of that state (Eq. 1) as one. $|\alpha\rangle$ and $|\beta\rangle$ are assigned to the computational basis states $|0\rangle$ and $|1\rangle$, thus Eq. (1) can be written as,

$$\begin{aligned}
\psi &= |010\dots\dots 0\rangle \\
\sigma &= |\psi\rangle\langle\psi| = I_1^0 I_2^1 I_3^0 \dots\dots I_n^0.
\end{aligned} \tag{3}$$

The algorithm aims to search a single object in $N = 2^n$ unsorted objects which are represented by 2^n basis states of 'n' qubits, which we call as work qubits. The density matrices of these states are represented in the Liouville space as,

$$\begin{aligned}
\sigma_1 &= I_1^0 I_2^0 I_3^0 \dots\dots I_n^0 = |0_1 0_2 0_3 \dots 0_n\rangle\langle 0_1 0_2 0_3 \dots 0_n|, \\
\sigma_2 &= I_1^0 I_2^0 I_3^0 \dots\dots I_{n-1}^0 I_n^1 = |0_1 0_2 0_3 \dots 0_{n-1} 1_n\rangle\langle 0_1 0_2 0_3 \dots 0_{n-1} 1_n| \\
&\vdots \\
\sigma_{2^n} &= I_1^1 I_2^1 I_3^1 \dots\dots I_n^1 = |1_1 1_2 1_3 \dots 1_n\rangle\langle 1_1 1_2 1_3 \dots 1_n|.
\end{aligned} \tag{4}$$

Let the marked state is σ_m ($m=1,2,\dots,2^n$). The algorithm uses an extra qubit known as ancilla qubit I_0 , and finds the marked object in 'n' ($= \log_2 N$) queries.

(i) **Preparation of initial states:** 'n' initial states, ρ_{in}^k ($k=1, 2, \dots, n$), are prepared in 'n' different experiments, ρ_{in}^k is given by [9, 12],

$$\begin{aligned}
\rho_{in}^k &= I_0^0 I_k^0 \\
&= I_0^0 [\mathbb{1}_1 \mathbb{1}_2 \dots \mathbb{1}_{k-1} I_k^0 \mathbb{1}_{k+1} \dots \mathbb{1}_n] \\
&= I_0^0 [(I_1^0 I_2^0 \dots I_{k-1}^0 I_k^0 I_{k+1}^0 \dots I_n^0) + (I_1^0 I_2^0 \dots I_{k-1}^0 I_k^0 I_{k+1}^0 \dots I_n^1) + \dots \\
&\quad + (I_1^1 I_2^1 \dots I_{k-1}^1 I_k^0 I_{k+1}^1 \dots I_n^1)] \\
&= I_0^0 [\sigma_1^k + \sigma_2^k + \dots + \sigma_{2^{n-1}}^k] = I_0^0 \sigma_{in}^k.
\end{aligned} \tag{5}$$

In Eq. (5), ancilla qubit and k^{th} work qubit are in state $|0\rangle$, whereas each of the remaining $(n-1)$ qubits are in state $|0\rangle$ or $|1\rangle$. Thus ρ_{in}^k has equal and non-zero populations (each of magnitude 1) in 2^{n-1} energy levels [9, 12]. In other words, all the matrix elements of ρ_{in}^k are zero, except for 2^{n-1} diagonal elements, each of which represent populations of value 1. The initial state ρ_{in}^k can be prepared in weakly coupled spins by using spin selective pulses and J-evolutions [12, 13].

In Eq. (5) since k^{th} work qubit of each σ_i^k , is already set to $|0_k\rangle$, if σ_{in}^k contains the marked state σ_m , then it implies that k^{th} work qubit of the marked state is $|0_k\rangle$. In other words $\sigma_m = I_1^{0/1} I_2^{0/1} \dots I_{k-1}^{0/1} \mathbf{I}_k^0 I_{k+1}^{0/1} \dots I_n^{0/1}$. If σ_{in}^k does not contain σ_m , then k^{th} work qubit of the marked state must be $|1_k\rangle$, that is $\sigma_m = I_1^{0/1} I_2^{0/1} \dots I_{k-1}^{0/1} \mathbf{I}_k^1 I_{k+1}^{0/1} \dots I_n^{0/1}$ [12, 13].

(ii) **Oracle:** Oracle is a black box, contents of which are unknown to the reader. Unitary operator (U) of oracle, inverts the states $I_0^0 \sigma_m$ and $I_0^1 \sigma_m$. The resultant state ρ_f^k is then given by,

$$\begin{aligned}
\rho_f^k &= U(\rho_{in}^k) = U(I_0^0 \sigma_{in}^k) = I_0^0 \sigma_{in}^k, \text{ if } \sigma_{in}^k \text{ does not contain the marked state } \sigma_m, I_k \Rightarrow I_k^1 \\
&= I_0^1 \sigma_m + I_0^0 [\sigma_{in}^k - \sigma_m], \\
&\quad \text{if } \sigma_{in}^k \text{ contains the marked state } \sigma_m, I_k \Rightarrow I_k^0.
\end{aligned} \tag{6}$$

As one can see in Eq. (6), 'U' is operated simultaneously on all the qubits of the ensemble.

(iii) Measurement: The ancilla qubit (I_0) is detected by applying a $(\pi/2)_y^0$ pulse on ρ_f^k [12]. The spectrum of I_0 contains 2^{n-1} peaks corresponding to 2^{n-1} states of σ_{in}^k . In Eq. (6), if $\rho_f^k = \rho_{in}^k$ then all the peaks are of positive intensity, which indicates that the k^{th} qubit of the marked state is in state $|1\rangle$ or $\sigma_m = I_1^{0/1} I_2^{0/1} \dots I_{k-1}^{0/1} \mathbf{1}_k I_{k+1}^{0/1} \dots I_n^{0/1}$ [9, 12]. If $\rho_f^k = I_0^1 \sigma_m - I_0^0 [\sigma_{in}^k - \sigma]$, then the spectrum contains a negative peak corresponding to σ_m , whereas remaining $(2^{n-1} - 1)$ peaks are of positive intensity, which indicates that $\sigma_m = I_1^{0/1} I_2^{0/1} \dots I_{k-1}^{0/1} \mathbf{0}_k I_{k+1}^{0/1} \dots I_n^{0/1}$ [12].

A sequence of 'n' experiments with input $\rho_{in}^k = I_0^0 I_k^0$, $k=1, 2, \dots, n$, are recorded. In the k^{th} experiment if all the peaks are positive then the marked state contains I_k^1 , otherwise it is I_k^0 [9]. Thus in 'n' experiments one can find the states of all the work qubits, I_1, I_2, \dots, I_n of the marked state.

3. GENERALIZED LIOUVILLE SPACE SEARCH ALGORITHM

Liouville space search algorithm has been implemented in NMR by using weakly J-coupled spins [12, 13]. Various steps of the algorithm are implemented by using qubit (spin) selective pulses and evolving the system under J-couplings [12, 13]. It is difficult to implement this algorithm in strongly coupled spins, since the spins are not individually addressable in the spectrum. Also it is difficult to manipulate the time evolution under a desired Hamiltonian. In other words eigen states are not the product states of individual spins. However an n-coupled system can be collectively treated as an n-qubit system, by treating the 2^n eigen states as computational basis states [21, 22, 23, 24]. In such systems it is difficult to apply qubit selective pulses, but one can still manipulate the states by applying transition selective pulses. Thus the original algorithm explained in section (2), is modified in such a way that various steps of the algorithm can be implemented by using transition selective pulses. The modified algorithm is implemented here in strongly coupled spins, but can be implemented

in weakly coupled spins as well.

Consider an $(n+1)$ -qubit system (weakly or strongly coupled), where the 2^{n+1} eigen states are labeled as $|0_0 0_1 \dots 0_n\rangle \dots \dots |1_0 1_1 \dots 1_n\rangle$, where the subscripts '0' and 1, 2, ..., n represent ancilla qubit and 'n' work qubits respectively. The search space contains 2^n states of 'n' work qubits, whose density matrices in 2^n - dimensional subspace of 2^{n+1} - dimensional eigen basis, are given by,

$$\begin{aligned}\sigma_1 &= |\psi_1\rangle\langle\psi_1| = |0_1 0_2 \dots 0_n\rangle\langle 0_1 0_2 \dots 0_n| \\ \sigma_2 &= |\psi_2\rangle\langle\psi_2| = |0_1 0_2 \dots 1_n\rangle\langle 0_1 0_2 \dots 1_n| \\ &\vdots \\ \sigma_{2^n} &= |\psi_{2^n}\rangle\langle\psi_{2^n}| = |1_1 1_2 \dots 1_n\rangle\langle 1_1 1_2 \dots 1_n|.\end{aligned}\tag{7}$$

In Eq. (7), the matrix elements of σ_i ($i = 1, 2, \dots, 2^n$) are zero, except for one diagonal element of value 1, which corresponds to the state ψ_i . The marked state is represented by,

$$\sigma_m = |\psi_m\rangle\langle\psi_m| = |x_1 x_2 \dots x_n\rangle\langle x_1 x_2 \dots x_n|, \text{ where } m=1, 2, \dots, 2^n \text{ and } x_i=0 \text{ or } 1.\tag{8}$$

(i) Preparation of initial states: 'n' initial states ρ_{in}^k ($k=1, 2, \dots, n$) are prepared in 'n' different experiments using the method of POPS (pair of pseudopure states) [19]. POPS(i, j) contains populations only in states $|i\rangle$ and $|j\rangle$, given by 'p' and '-p' respectively, where the value of 'p' depends on the details of preparation [19]. POPS(i, j) can be achieved by inverting the populations of a pair of states $|i\rangle$ and $|j\rangle$ and subtracting the resultant population distribution from that of equilibrium state [19].

In each initial state ρ_{in}^k , ancilla and k^{th} work qubits are in state $|0\rangle$, whereas each of the remaining $(n-1)$ qubits are in state 0 or 1. Thus the initial state contains non zero populations in 2^{n-1} states, also for every state of population p_i^k there exist another state of population of $-p_i^k$. In other words, ρ_{in}^k is a sum of $(2^{n-1}/2)$ POPS, thus it represents a highly mixed state. ρ_{in}^k is prepared by subtracting ρ_k from ρ_{eq} (equilibrium populations),

where ρ_k is obtained by inverting the populations of $(2^{n-1}/2)$ pairs of states, and subtracting the resultant population distribution from that of equilibrium state, ρ_{in}^k is given by,

$$\begin{aligned}
\rho_{in}^k &= \rho_{eq} - \rho_k, \\
&= p_1^k |\mathbf{0}_0 0_1 0_2 \dots 0_{k-1} \mathbf{0}_k 0_{k+1} \dots 0_n\rangle \langle \mathbf{0}_0 0_1 0_2 \dots \mathbf{0}_k \dots 0_n| \\
&\quad + p_2^k |\mathbf{0}_0 0_1 0_2 \dots 0_{k-1} \mathbf{0}_k 0_{k+1} \dots 1_n\rangle \langle \mathbf{0}_0 0_1 0_2 \dots 0_{k-1} \mathbf{0}_k 0_{k+1} \dots 1_n| \\
&\quad + \dots \dots \dots + p_{2^{n-1}}^k |\mathbf{0}_0 1_1 1_2 \dots 1_{k-1} \mathbf{0}_k 1_{k+1} \dots 1_n\rangle \langle \mathbf{0}_0 1_1 1_2 \dots 1_{k-1} \mathbf{0}_k 1_{k+1} \dots 1_n| \\
&= p_1^k |0_0 \psi_1^k\rangle \langle 0_0 \psi_1^k| + p_2^k |0_0 \psi_2^k\rangle \langle 0_0 \psi_2^k| + \dots \dots \dots + p_{2^{n-1}}^k |0_0 \psi_{2^{n-1}}^k\rangle \langle 0_0 \psi_{2^{n-1}}^k|, \tag{9}
\end{aligned}$$

where $p_1^k, p_2^k, \dots, p_{2^{n-1}}^k$ represent the populations in the respective levels, and for every p_i^k there exists a $-p_i^k$, thus ρ_{in}^k represents a sum of $(2^{n-1}/2)$ POPS. In Eq. (9) the k^{th} work qubit is set in state $|0_k\rangle$, hence if ρ_{in}^k contains the marked state $|\psi_m\rangle = |x_1 x_2 \dots x_k \dots x_n\rangle$, it implies that the k^{th} work qubit of $|\psi_m\rangle$ that is $x_k = 0$, whereas if ρ_{in}^k does not contain $|\psi_m\rangle$ then $x_k = 1$.

(ii) Oracle: The unitary operator of the oracle acting on ρ_{in}^k , flips the states $|0_0 \psi_m\rangle$ and $|1_0 \psi_m\rangle$. 'U' can be implemented by applying a selective (π) pulse on transition $|0_0 \psi_m\rangle \Leftrightarrow |1_0 \psi_m\rangle$. The final state ρ_f^k is given by,

$$\begin{aligned}
\rho_f^k &= U(\rho_{in}^k) = \rho_{in}^k, \text{ if } \rho_{in}^k \text{ does not contain the marked state } |\psi_m\rangle \Rightarrow x_k=1 \\
&= p_m^k |1_0 \psi_m\rangle \langle 1_0 \psi_m| + (\rho_{in}^k - p_m^k |0_0 \psi_m\rangle \langle 0_0 \psi_m|), \\
&\quad \text{if } \rho_{in}^k \text{ contains the marked state } |\psi_m\rangle \Rightarrow x_k=0. \tag{10}
\end{aligned}$$

(iii) Measurement: A multi frequency $(\pi/2)_y$ pulse is applied on 2^n unconnected transitions (ancilla qubit transitions) corresponding to 2^n pairs of states $|0_0 i_1 i_2 \dots i_n\rangle \Leftrightarrow |1_0 i_1 i_2 \dots i_n\rangle$, where $i_1, i_2, \dots, i_n = 0$ or 1 , followed by the detection. In case of weakly coupled system with conventional labeling (that is the states $|\alpha\rangle$ and $|\beta\rangle$ of each spin, represent $|0\rangle$ and $|1\rangle$ respectively), these 2^n transitions belong to I_0 qubit. Hence the read-out pulse

is selective $(\pi/2)_y$ pulse on I_0 qubit. Thus in case of weakly coupled spins, measurement strategy is same as that of the original algorithm [9, 12], [section 2].

In Eq. (10), if the final state $\rho_f^k = \rho_{in}^k$, then the MF pulse converts the populations $p_1^k |0_0 \psi_1^k\rangle \langle 0_0 \psi_1^k|$, $p_2^k |0_0 \psi_2^k\rangle \langle 0_0 \psi_2^k|$, $p_{2^{n-1}}^k |0_0 \psi_{2^{n-1}}^k\rangle \langle 0_0 \psi_{2^{n-1}}^k|$, to 2^{n-1} coherences. Since for every p_i^k there exists $-p_i^k$, number of positive transitions (associated with positive p_i^k) is equal to number of negative transitions (associated with negative p_i^k). If ρ_f^k contains the marked state (corresponds to second equality of Eq. 10), then positive and negative populations (other than $p_m^k |1_0 \psi_m\rangle \langle 1_0 \psi_m|$) are converted in to positive and negative transitions respectively, whereas a positive or negative $p_m^k |1_0 \psi_m\rangle \langle 1_0 \psi_m|$ gives a negative or positive peak respectively. Thus, if ρ_f^k contains the marked state, then spectrum contains $(2^{n-1}/2) \pm 1$ positive peaks and $(2^{n-1}/2) \mp 1$ negative peaks, where + and - respectively corresponds to negative and positive p_m^k .

In summary, in the k^{th} experiment with initial state ρ_{in}^k , if the spectrum of final state contains equal number of positive and negative peaks, then the k^{th} work qubit is in state $|1\rangle$ or $x_k = 1$. Whereas if the spectrum contains unequal number of positive and negative peaks then $x_k = 0$. This procedure is repeated for each of the 'n' initial states ρ_{in}^k ($k=1,2,\dots,n$), then one obtains the marked state $\sigma_m = |x_1 x_2 \dots x_n\rangle \langle x_1 x_2 \dots x_n|$.

It is to be noted that, since $\rho_{in}^k = \rho_{eq} - \rho_k$ (Eq. 9), implementation of 'U' and measurement are performed in different experiments for ρ_{eq} and ρ_k ($k = 1, 2, \dots, n$). Now the spectrum of ρ_f^k is obtained by subtracting the final spectrum of ρ_k from that of ρ_{eq} . Thus the total number of experiments is $(n+1)$.

4. EXPERIMENTAL IMPLEMENTATION ON A STRONGLY DIPOLAR COUPLED 4-QUBIT SYSTEM

The system chosen is, four protons of 2-chloro, iodo benzene oriented in ZLI-1132 liquid crystal [22]. The four protons are strongly coupled to each other through dipolar couplings,

and contains 16 eigen states. The total Hamiltonian of the system contains, chemical shift (H_c), dipolar (H_{DD}), and J-coupling (H_J) terms, given by,

$$H = H_c + H_{DD} + H_J = \sum_{i=1}^4 \omega_i I_{iz} + \sum_{i,j=1, \text{ and } i < j}^4 [2\pi D_{ij}(3I_{iz}I_{jz} - I_i \cdot I_j) + 2\pi J_{ij}I_i \cdot I_j]. \quad (11)$$

Experiments are carried out on AV-500 NMR spectrometer. Figure (1) shows the 1H 1D spectrum obtained by applying a hard $(\pi/2)_y$ pulse. In order to perform the Liouville search, one needs to know the pair of states from which each transition originates or in other words, we need to know the complete energy level diagram of the spin system. The energy level diagram of this system, has been obtained by Mahesh et al, using the connectivity information from Z-COSY experiment [22]. The pulse sequence of a Z-COSY experiment is, $90^\circ - t_1 - \alpha - \tau - \beta - t_2$, where only the longitudinal magnetization is retained during the interval τ by either phase cycling or by a gradient pulse [23, 26]. The 90° pulse converts the equilibrium z -magnetization into coherences, which are frequency labeled during the period t_1 . The small angle α pulse ensures that each cross-section parallel to ω_2 from the resulting 2D spectrum is equivalent to a one-dimensional (1D) experiment in which the peak corresponding to the diagonal is selectively inverted [26]. The directly connected transitions to the inverted transition are finally measured in the linear regime by a small angle β pulse. Figure (2) shows the energy level diagram of this system, obtained from Z-COSY experiment [22], where each of the transitions of Fig. (1) are assigned to a pair of energy levels.

The 16 eigen states (Fig. 2) are labeled as computational basis states of a four qubit system, given by, $|0_00_10_20_3\rangle, |0_00_10_21_3\rangle, \dots, |1_01_11_21_3\rangle$, where the subscripts '0' and 1, 2, 3 represent ancilla qubit and three work qubits. It is to be noted that the labeling of eigen states shown in Fig. (2), is different from that of ref. [22]. The labeling in our case follows two strategies: (i) Find eight unconnected transitions, and label the eigen states such that these transitions belong to ancilla qubit. In other words, each of the eight transitions is associated with a pair of states $|0_0i_1i_2i_3\rangle \Leftrightarrow |1_0i_1i_2i_3\rangle$, where $i_1i_2i_3 = 000, 001, \dots, 111$; the states

$|0_0i_1i_2i_3\rangle$ and $|1_0i_1i_2i_3\rangle$ respectively represent the lower and upper states of the transition. However in this system we could find only seven unconnected transitions, represented by dark lines in Fig. (2), the transition between the states $|0_01_11_21_3\rangle \Leftrightarrow |1_01_11_21_3\rangle$ is not observed due to low intensity. (ii) The initial states ρ_{in}^k (Eq. 13) contain the eigen states $|0000\rangle, |0001\rangle, |0010\rangle, |0100\rangle, |0011\rangle$ and $|0101\rangle$, hence to prepare ρ_{in}^k each of these states should not be isolated from the rest of eigen states, for example the labeling of any of these eigen states can not be interchanged with that of $|0111\rangle$ since this state is isolated (Fig. 2). Following these two criteria there exists many possibilities of labeling these eigen states, the present being one of them. It may be pointed out that the second strategy is not necessary, if none of the states are isolated.

Liouville space search is now performed, following the procedure given in section (3). The search space contains eight states of the work qubits, given by,

$$\begin{aligned}
\sigma_1 &= |\psi_1\rangle\langle\psi_1| = |0_10_20_3\rangle\langle 0_10_20_3|, & \sigma_2 &= |\psi_2\rangle\langle\psi_2| = |0_10_21_3\rangle\langle 0_10_21_3| \\
\sigma_3 &= |\psi_3\rangle\langle\psi_3| = |0_11_20_3\rangle\langle 0_11_20_3|, & \sigma_4 &= |\psi_4\rangle\langle\psi_4| = |0_11_21_3\rangle\langle 0_11_21_3| \\
\sigma_5 &= |\psi_5\rangle\langle\psi_5| = |1_10_20_3\rangle\langle 1_10_20_3|, & \sigma_6 &= |\psi_6\rangle\langle\psi_6| = |1_10_21_3\rangle\langle 1_10_21_3| \\
\sigma_7 &= |\psi_7\rangle\langle\psi_7| = |1_11_20_3\rangle\langle 1_11_20_3|, & \text{and } \sigma_8 &= |\psi_8\rangle\langle\psi_8| = |1_11_21_3\rangle\langle 1_11_21_3|.
\end{aligned}
\tag{12}$$

Let the marked state is $\sigma_6 = |\psi_6\rangle\langle\psi_6|$.

(i) Preparation of initial states:

Three initial states ρ_{in}^k ($k=1, 2, 3$) are required since there are three work qubits. From Eq. (9) we can write these initial states as,

$$\begin{aligned}
\rho_{in}^1 &= p_1^1 |0_0 0_1 0_2 0_3\rangle \langle 0_0 0_1 0_2 0_3| + p_2^1 |0_0 0_1 0_2 1_3\rangle \langle 0_0 0_1 0_2 1_3| \\
&\quad + p_3^1 |0_0 0_1 1_2 0_3\rangle \langle 0_0 0_1 1_2 0_3| + p_4^1 |0_0 0_1 1_2 1_3\rangle \langle 0_0 0_1 1_2 1_3| \\
\rho_{in}^2 &= p_1^2 |0_0 0_1 0_2 0_3\rangle \langle 0_0 0_1 0_2 0_3| + p_2^2 |0_0 0_1 0_2 1_3\rangle \langle 0_0 0_1 0_2 1_3| \\
&\quad + p_3^2 |0_0 1_1 0_2 0_3\rangle \langle 0_0 1_1 0_2 0_3| + p_4^2 |0_0 1_1 0_2 1_3\rangle \langle 0_0 1_1 0_2 1_3| \\
\rho_{in}^3 &= p_1^3 |0_0 0_1 0_2 0_3\rangle \langle 0_0 0_1 0_2 0_3| + p_2^3 |0_0 0_1 0_2 1_3\rangle \langle 0_0 0_1 0_2 1_3| \\
&\quad + p_3^3 |0_0 1_1 0_2 0_3\rangle \langle 0_0 1_1 0_2 0_3| + p_4^3 |0_0 1_1 0_2 1_3\rangle \langle 0_0 1_1 0_2 1_3|.
\end{aligned} \tag{13}$$

In each experiment, for every p_i^k there exists another population which is $-p_i^k$.

A density matrix ρ_1 is prepared from ρ_{eq} (Fig. 2), by applying a selective π pulse on transition (23) which interchanges the populations of $|0_0 0_1 0_2 0_3\rangle$ & $|0_0 0_1 1_2 0_3\rangle$, and a cascade of π pulses on (30), (9) and (30) which interchanges the populations of $|0_0 0_1 0_2 1_3\rangle$ & $|0_0 0_1 1_2 1_3\rangle$. Now ρ_{in}^1 is obtained by subtracting ρ_1 from ρ_{eq} , the resultant populations of ρ_{in}^1 are shown in Fig. (3), which can also be written as,

$$\begin{aligned}
\rho_{in}^1 &= \rho_{eq} - \rho_1 = |0_0 0_1 0_2 0_3\rangle \langle 0_0 0_1 0_2 0_3| + 2|0_0 0_1 0_2 1_3\rangle \langle 0_0 0_1 0_2 1_3| \\
&\quad - |0_0 0_1 1_2 0_3\rangle \langle 0_0 0_1 1_2 0_3| - 2|0_0 0_1 1_2 1_3\rangle \langle 0_0 0_1 1_2 1_3|.
\end{aligned} \tag{14}$$

Figure (4a) shows the spectrum of ρ_{in}^1 (Fig. 3), obtained by subtracting the spectrum of ρ_1 from ρ_{eq} , where each of the spectra of ρ_1 and ρ_{eq} were recoded by applying a 5° pulse. In Fig. (3), the population difference corresponding to transitions (29), (24), (23), (27), (30), (25) and (9) are positive, while those of (16), (22), (28), (14) and (1) are negative. This is confirmed from the spectrum of Fig. (4a), the transitions (14) and (16) are not visible due to low intensity.

The ρ_{in}^2 is given by,

$$\begin{aligned} \rho_{in}^2 = \rho_{eq} - \rho_2 = & |0_00_10_20_3\rangle\langle 0_00_10_20_3| + |0_00_10_21_3\rangle\langle 0_00_10_21_3| \\ & - |0_01_10_20_3\rangle\langle 0_01_10_20_3| - |0_01_10_21_3\rangle\langle 0_01_10_21_3|, \end{aligned} \quad (15)$$

where ρ_2 is obtained from ρ_{eq} (Fig. 2), by applying six selective π pulses on transitions (24), (30), (21), (5), (21) and (30) respectively, where the first pulse inverts the populations of $|0_00_10_20_3\rangle$ & $|0_01_10_20_3\rangle$ and next five pulses invert the populations of $|0_00_10_21_3\rangle$ & $|0_01_10_21_3\rangle$. Figure (5) shows the population distribution of ρ_{in}^2 and the corresponding spectrum is shown in Fig. (4b). The positive and negative transitions in Fig. (4b) are in accordance with the population distribution of Fig. (5).

Similarly one obtains,

$$\begin{aligned} \rho_{in}^3 = \rho_{eq} - \rho_3 = & |0_00_10_20_3\rangle\langle 0_00_10_20_3| + |0_00_11_20_3\rangle\langle 0_00_11_20_3| \\ & - |0_01_10_20_3\rangle\langle 0_01_10_20_3| - |0_01_11_20_3\rangle\langle 0_01_11_20_3|, \end{aligned} \quad (16)$$

where ρ_3 prepared from ρ_{eq} (Fig. 2), by applying two selective π pulses on transitions (24) and (22) which invert the populations of $|0_00_10_20_3\rangle$ & $|0_01_10_20_3\rangle$ and $|0_00_11_20_3\rangle$ & $|0_01_11_20_3\rangle$ respectively. Figure (4c) shows the spectrum of ρ_{in}^3 which reflects the population distribution of Fig. (6).

(ii) Oracle: To search the state $|\psi_6\rangle$ (Eq. 12), the unitary operator (U) of oracle, interchanges the states $|0_0\psi_6\rangle$ and $|1_0\psi_6\rangle$. Here U is achieved by applying a selective π pulse on transition (18). The resultant states ρ_f^1 , ρ_f^2 and ρ_f^3 are given by,

$$\begin{aligned}
\rho_f^1 &= U(\rho_{in}^1) = U(\rho_{eq}) - U(\rho_1) = \rho_{in}^1 \\
\rho_f^2 &= U(\rho_{in}^2) = U(\rho_{eq}) - U(\rho_2) \\
&= U(|0_00_10_20_3\rangle\langle 0_00_10_20_3|) + U(|0_00_10_21_3\rangle\langle 0_00_10_21_3|) - U(|0_01_10_20_3\rangle\langle 0_01_10_20_3|) \\
&\quad - U(|0_01_10_21_3\rangle\langle 0_01_10_21_3|) \\
&= |0_00_10_20_3\rangle\langle 0_00_10_20_3| + |0_00_10_21_3\rangle\langle 0_00_10_21_3| - |0_01_10_20_3\rangle\langle 0_01_10_20_3| \\
&\quad - (|1_01_10_21_3\rangle\langle 1_01_10_21_3|) \\
\rho_f^3 &= U(\rho_{in}^3) = U(\rho_{eq}) - U(\rho_3) = \rho_{in}^3.
\end{aligned} \tag{17}$$

In Eq. (17), U converts the state $|0_01_10_21_3\rangle$ of ρ_{in}^2 in to $|1_01_10_21_3\rangle$, whereas ρ_{in}^1 and ρ_{in}^3 are not effected by U, since neither of these states contain either $|0_01_10_21_3\rangle$ or $|1_01_10_21_3\rangle$.

(iii) Measurement: Measurement requires a multi frequency $(\pi/2)_y$ on eight unconnected ancilla qubit transitions of the final state (ρ_f^k) followed by the detection. The eight transitions of MF pulse correspond to eight pairs energy levels, $|0_0i_1i_2i_3\rangle \Leftrightarrow |1_0i_1i_2i_3\rangle$, where $i_1, i_2, i_3 = 0$ or 1. The transition between the energy levels $|0_01_11_21_3\rangle$ and $|1_01_11_21_3\rangle$ is not observed in the Z-COSY assignment of Fig. (1) [22], due to low intensity. However this transition is not required, since it any way gives rise to zero intensity peak, because the final states ρ_f^k after the oracle of search state $|\psi_6\rangle$ (Eq. 17) and also for remaining search states, contain zero populations in $|0_01_11_21_3\rangle$ and $|1_01_11_21_3\rangle$. Hence the multi frequency $(\pi/2)$ pulse is applied on remaining seven transitions, (1), (8), (10), (18), (27), (28), (29) (represented by dark lines in Figs 3, 5, 6). The duration of MF pulse is 70 ms, which is obtained by modulating the Gaussian pulse with seven harmonics corresponding to these seven transitions, the phase of each harmonic is 'y'. The amplitude of each harmonic is adjusted such that the pulse gives maximum intensity for each transition, in other words, the MF pulse corresponds to a $(\pi/2)_y$ pulse on each of the seven transitions. The spectra of ρ_f^1 , ρ_f^2 and ρ_f^3 are given in Figs 7 (a), (b) and (c) respectively. In Figs (7a, c) number of positive peaks is equal to number of negative peaks, hence the first and third qubits of the

marked state, are in state $|1\rangle$. Whereas in Fig. (7b), number of positive peaks is not equal to number of negative peaks, hence second work qubit is in state $|0\rangle$. Thus the marked is $|1_1 0_2 1_3\rangle$.

It may be pointed out that, since the ancilla qubit transition $|0111\rangle \Leftrightarrow |1111\rangle$ is not observed (Fig. 1, 2), one can not perform the Oracle operation (U), to search the state $|111\rangle$ with the present labeling scheme.

5. CONCLUSIONS

In order to increase the number of qubits, one has to exploit the dipolar couplings among the spins, in which case the spins are often strongly coupled to each other. Unlike weakly coupled systems, strongly coupled systems can not be directly used for implementing quantum algorithms. In this work, we generalize the Liouville space search algorithm, such that it can be implemented in weakly as well as strongly coupled systems. Experimental implementation is carried out on a strongly dipolar coupled four qubit system. All the steps of the algorithm are implemented by using transition selective pulses.

-
- [1] M.A. Nielsen , I.L. Chuang. "*Quantum Computation and Quantum Information*", Cambridge University Press, Cambridge, U.K. 2000.
 - [2] A. M. Turing, *On computable numbers with an application to the Entscheidungsproblem*, Proc. London Math.Soc. **42**, 230 (1936).
 - [3] A. Church, *An unsolvable problem of elementary number theory*, *Am. J. Math.*, Am. J. Math. **58**, 345 (1936).
 - [4] D. Deutsch and R. Jozsa, *Rapid solution of problems by quantum computation*, Proc. R. Soc. Lond. A, **439**, 553 (1992).
 - [5] D. P. DiVincenzo, *Quantum computation*, Science **270**, 255, (1995).
 - [6] L.K. Grover, *Quantum Mechanics helps in searching for a needle in haystack*, Phys. Rev. Lett. **79**, 325 (1997).
 - [7] P. W. Shor, *Polynomial-time algorithms for prime factorization and discrete algorithms on quantum computer*, SIAM Rev, **41**, 303-332 (1999).
 - [8] Z. L. Madi, R. Bruschiweiler, and R. R. Ernst, *One- and two-dimensional ensemble quantum computing in spin Liouville space*, J. Chem. Phys. **109**, 10603 (1998).
 - [9] R. Bruschiweiler, *Novel Strategy for Database Searching in Spin Liouville Space by NMR Ensemble Computing*, Phys. Rev. Lett. **85**, 4815(2000).
 - [10] C. Dhelon and V. Protopopescu, *Journal of Physics A: Mathematical and General* **35**, pp. L597-L604 (2002).
 - [11] V. Protopopescu, C. DHelon, and J. Barhen *Journal of Physics A* **36** L399 (2003).
 - [12] L. Xiao, G. L. Long, H. Y. Yan, and Y. Sun, *Experimental realization of the Brschweiler's algorithm in a homonuclear system*, J. Chem. Phys. **117**, 3310 (2002).
 - [13] G. L. Long, L. Xiao, *Experimental realization of a fetching algorithm in a 7-qubit NMR spin Liouville space computer*, J. Chem. Phys. **119**, 8473 (2003).

- [14] L. Xiao, and G. L. Long, *Fetching marked items from an unsorted database in NMR ensemble computing*, Phys. Rev. A **66**, 052320 (2002).
- [15] G. L. Long, L. Xiao, *Parallel quantum computing in a single ensemble quantum computer*, Phys. Rev. A **69**, 052303 (2004).
- [16] J. A. Jones, *NMR quantum computation*, progress in NMR spectroscopy **38**, 325 (2001).
- [17] L. M. K. Vandersypen and I. L. Chuang, *NMR techniques for quantum control and computation*, Review of Modern Physics **76**, 1037 (2004).
- [18] R. R. Ernst, G. Bodenhausen, and A. Wokaun, *Principles of Nuclear Magnetic Resonance in One and Two Dimensions*, Oxford University Press (1987)
- [19] B. M. Fung, *Use of pairs of pseudopure states for NMR quantum computing*, Phys. Rev. A **63**, 022304 (2001).
- [20] A. K. Khitrin and B. M. Fung, *Nuclear magnetic resonance quantum logic gates using quadrupolar nuclei*, J. Chem. Phys. **112**, 6963 (2000).
- [21] T. S. Mahesh, Neeraj Sinha, K. V. Ramanathan, and Anil Kumar, *Ensemble quantum-information processing by NMR: Implementation of gates and the creation of pseudopure states using dipolar coupled spins as qubits*, Phys. Rev. A **65**, 022312 (2002).
- [22] T. S. Mahesh, Neeraj Sinha, Arindam Ghosh, Ranabir Das, N.Suryaprakash, Malcom H.Levitt, K. V. Ramanathan, and Anil Kumar, *Quantum information processing by NMR using strongly coupled spins*, Current Science **85**, 932 (2003); xxx.lanl.gov/abs/quant-ph/0212123.
- [23] Ranabir Das and Anil Kumar, *Quantum information processing by NMR using a 5-qubit system formed by dipolar coupled spin s in an oriented molecule*, J. Magn. Reson. **170** 310 (2004).
- [24] Jae-Seung Lee and A. K. Khitrin, *Pseudopure state of a twelve-spin system*, J. Chem. Phys **122**, 041101 (2005).
- [25] T. S. Mahesh and Dieter Suter, *Quantum-information processing using strongly dipolar coupled*

nuclear spins, Phys. Rev. A **74**, 062312 (2006).

- [26] R. C. R. Grace and Anil Kumar, *Flip angle dependence of non-equilibrium states yielding information on connectivity of transitions and energy levels of oriented molecules*, J. Magn. Reson. **99**, 81 (1992).

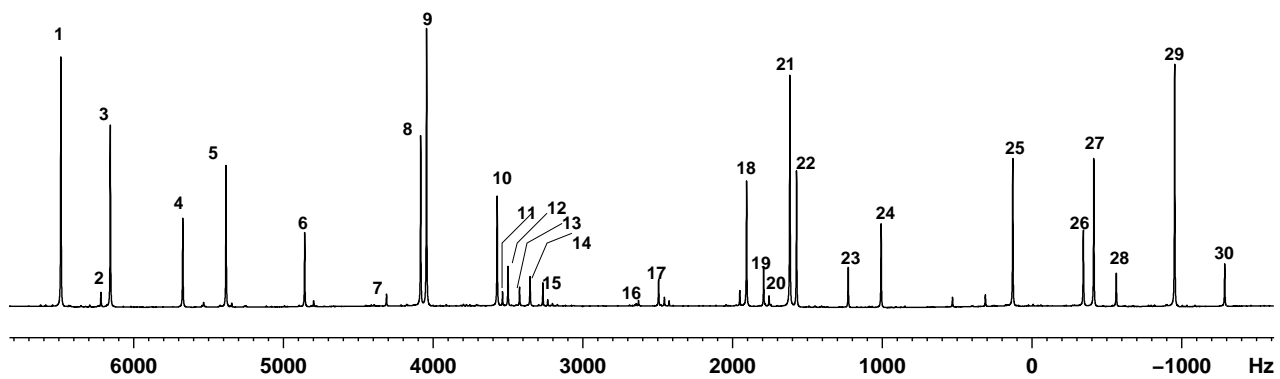


FIG. 1: ^1H equilibrium spectrum of 2-chloro, iodo benzene oriented in ZLI-1132 liquid crystal, recorded at room temperature (300k) on a 500 MHz NMR spectrometer. The four protons of the molecule are strongly dipolar coupled to each other. Various transitions are numbered in increasing order from left to right (decreasing frequency).

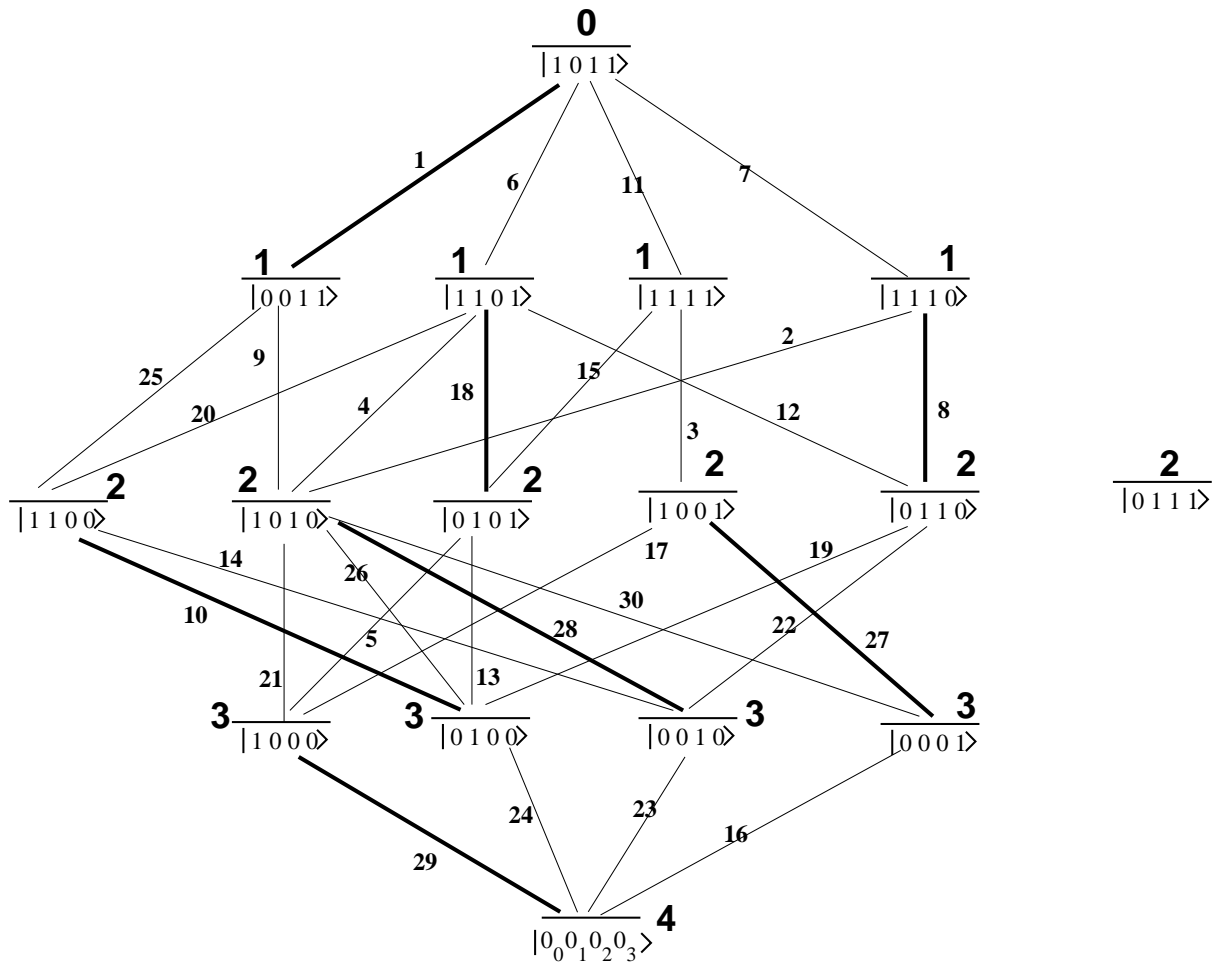


FIG. 2: Energy level diagram of oriented 2-chloro, iodo benzene, obtained by investigating the connectivity of various transitions of Fig. 1 by using a Z-COSY experiment [22]. The equilibrium populations (ρ_{eq}) of various levels (represented by bold numbers) are proportional to the Zeeman energies of the protons, schematically represented by the energy level diagram. The 16 eigen states are labeled as basis states of a four qubit system. The strategy adopted for this labeling scheme is explained in the text. The transitions represented by dark lines, correspond to ancilla (zeroth) qubit.

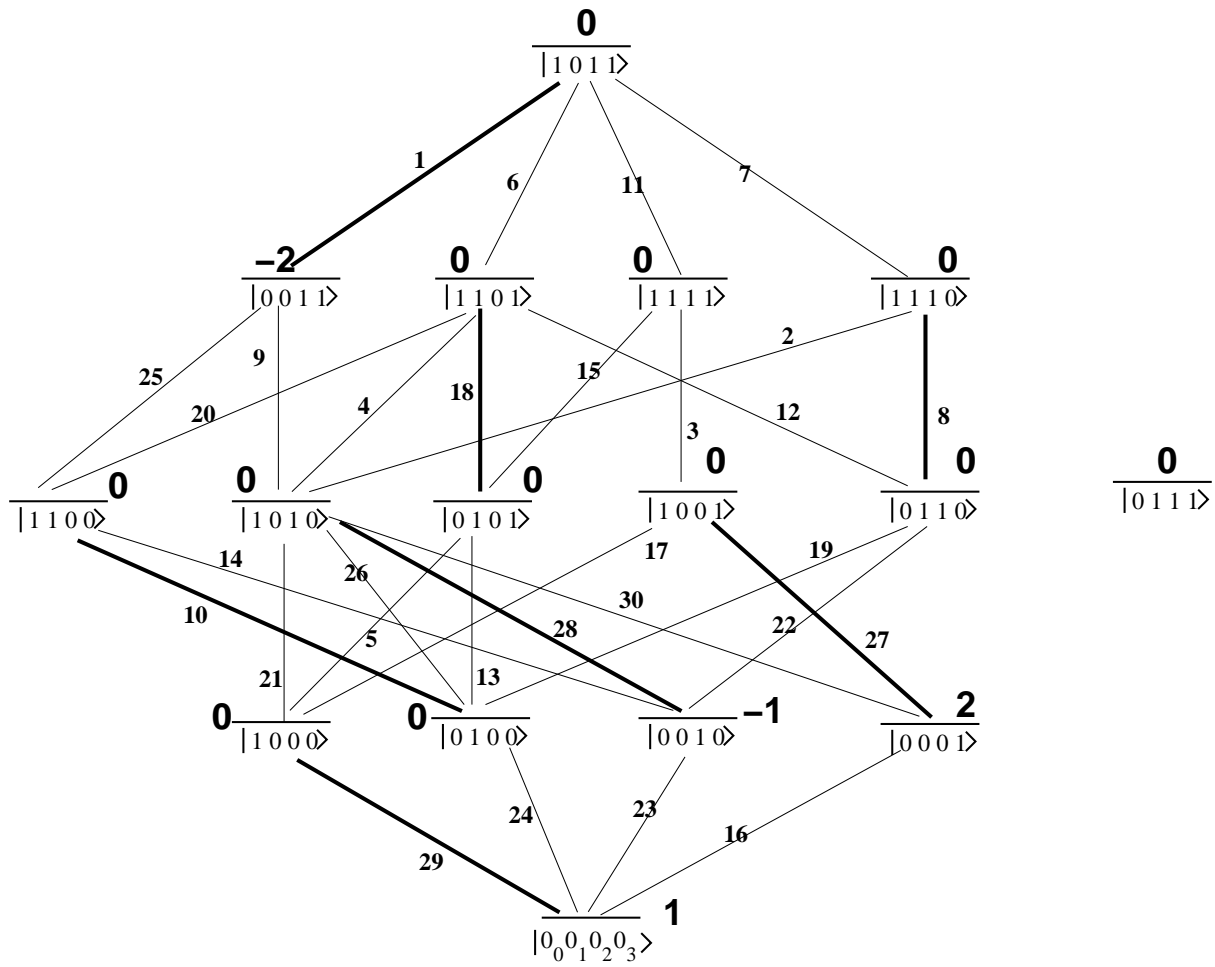


FIG. 3: Energy level diagram of Fig. (2), with the populations of various states corresponding to ρ_{in}^1 (Eq. 14). The transitions represented by dark lines, correspond to ancilla qubit.

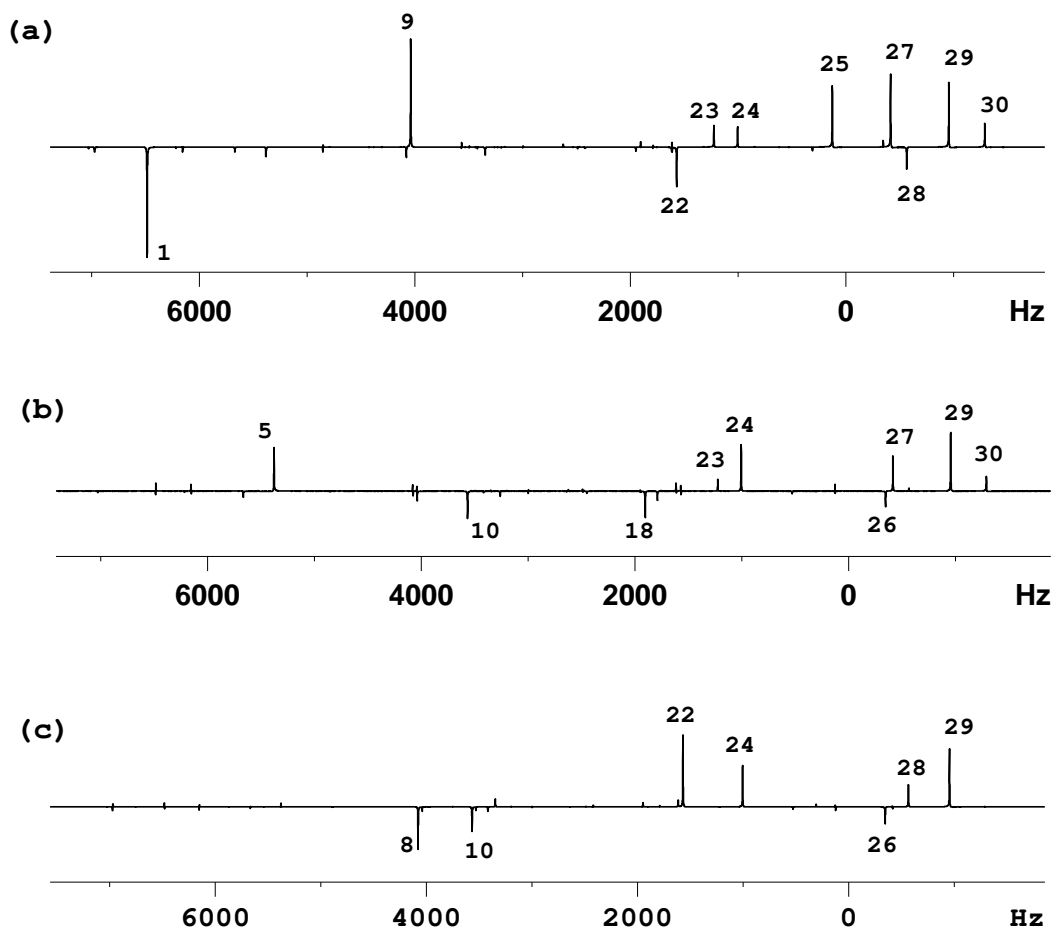


FIG. 4: The spectra of (a), (b) and (c) respectively represent the population distributions of ρ_{in}^1 (Fig. 3), ρ_{in}^2 (Fig. 5) and ρ_{in}^3 (Fig. 6). (a), (b) and (c) are respectively obtained by subtracting the spectra (recorded with 5° pulse) of ρ_1 , ρ_2 and ρ_3 from equilibrium (ρ_{eq}) spectrum (also recorded with a 5° pulse). Preparation of ρ_1 , ρ_2 and ρ_3 are explained in the text. Some small intensities such as 14 & 16 in (a), are not observed/marked.

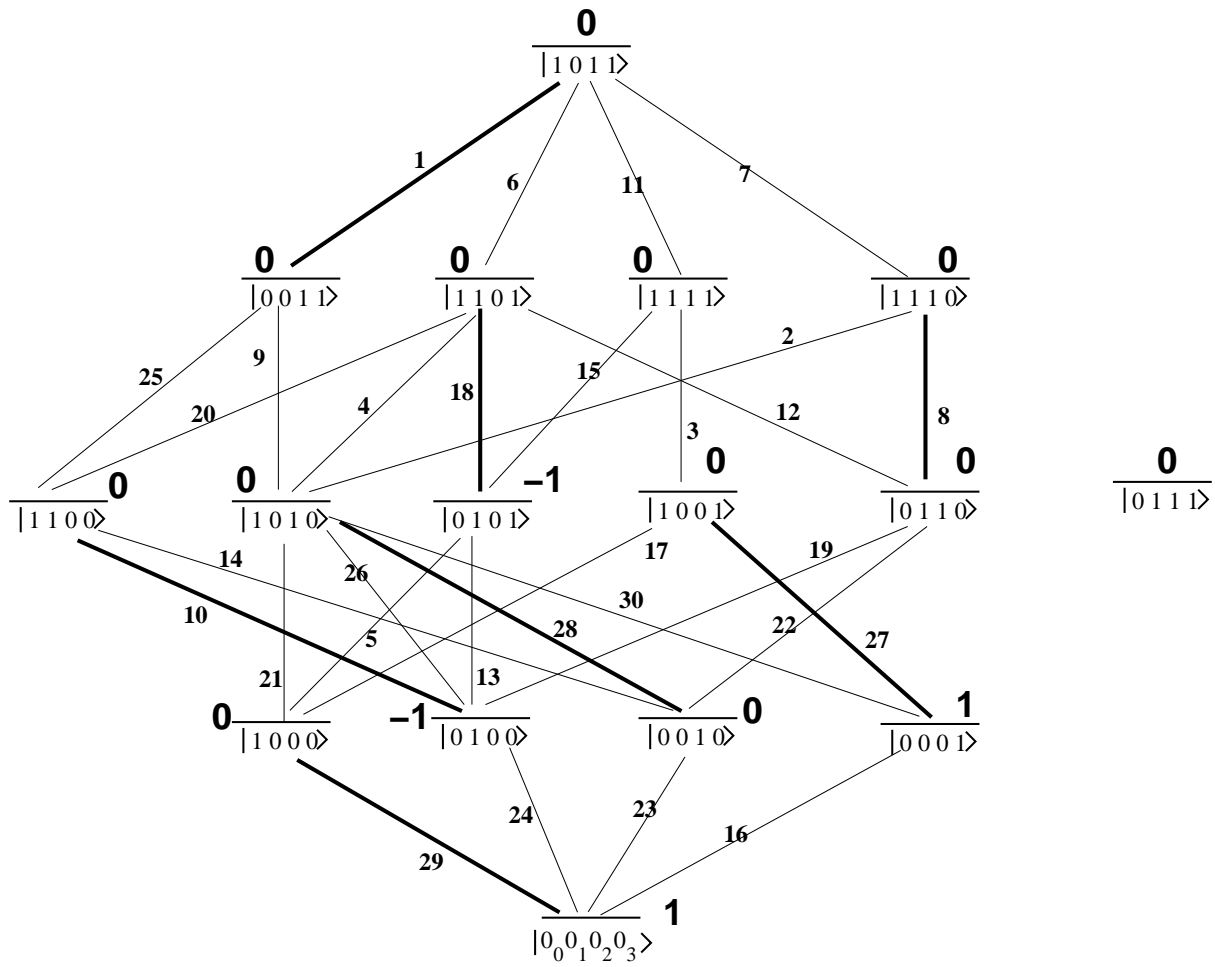


FIG. 5: Energy level diagram of Fig. (2), with the populations of various states corresponding to ρ_{in}^2 (Eq. 15), and the transitions represented by dark lines, correspond to ancilla qubit

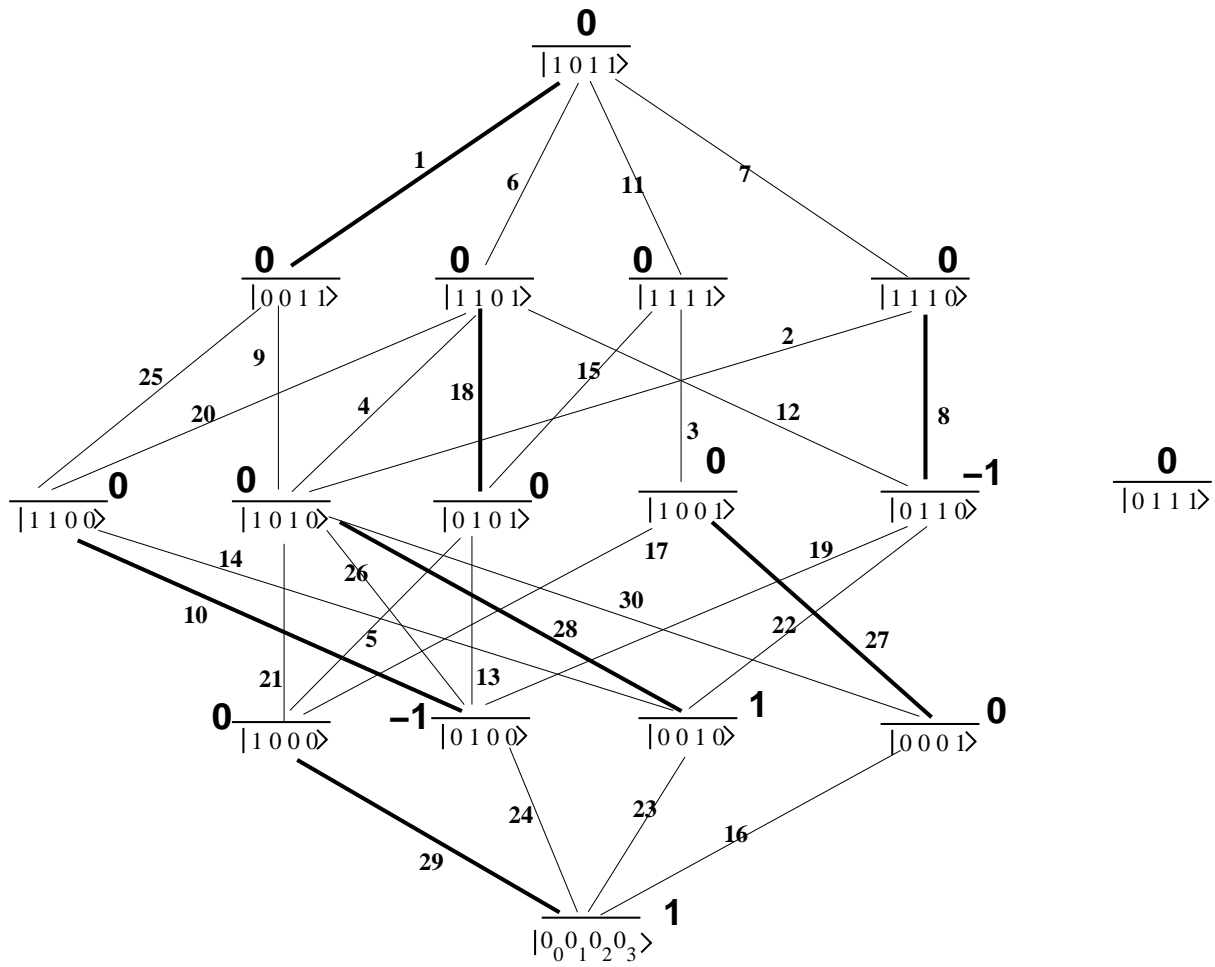


FIG. 6: Energy level diagram of Fig. (2), where the populations of various states correspond to ρ_{in}^3 (Eq. 16). The transitions represented by dark lines, correspond to ancilla qubit

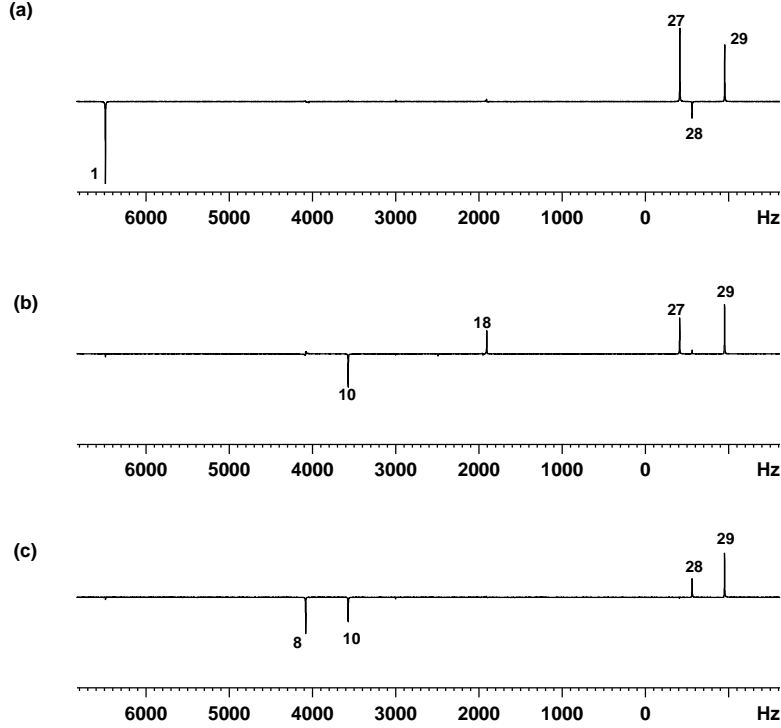


FIG. 7: Implementation of Generalized Liouville space search algorithm on a dipolar coupled four qubit system. The spectra of $U(\rho_{eq})$, $U(\rho_1)$, $U(\rho_2)$ and $U(\rho_3)$ (Eq. 17) are first obtained by applying a multi frequency pulse on ancilla qubit transitions (1), (8), (10), (18), (27), (28) and (29). Then the spectra (a), (b) and (c) are respectively obtained by subtracting the spectra of $U(\rho_1)$, $U(\rho_2)$ and $U(\rho_3)$ from $U(\rho_{eq})$ spectrum. (a), (b) and (c) thus respectively represent the ancilla qubit spectra of ρ_f^1 , ρ_f^2 and ρ_f^3 (Eq. 17). Since $\rho_f^1 = \rho_{in}^1$ and $\rho_f^3 = \rho_{in}^3$, the signs of ancilla qubit transitions of (a) and (c) are respectively equivalent to that of Fig. s (4a) and (4c), whereas in (b) of ρ_f^2 the sign of transition (8) is changed from that of ρ_{in}^2 Fig. (4b), due to the oracle operation. Thus the spectra of ρ_f^1 and ρ_f^3 (a,c) contains equal number of positive and negative peaks, whereas the spectrum of ρ_f^2 (b) contains unequal number of positive and negative peaks. Thus the search state is $|101\rangle$.